Macromolecules **2007,** *40,* 8897−8905

Atom Transfer Radical Dispersion Polymerization in an Ethanol/Water Mixture

Wen-Ming Wan and Cai-Yuan Pan*

Department of Polymer Science and Engineering, University of Science and Technology of China, Hefei, Anhui, 230026, P. R. China

Received June 10, 2007; Revised Manuscript Received September 2, 2007

ABSTRACT: The atom transfer radical dispersion polymerization of 4-vinylpyridine (4VP) in an ethanol/H_2O mixture displayed two stages of polymerization; the first stage is the formation of a diblock copolymer with the polymerization rate of 1.21 mol·L^{-1}·h^{-1} before 1 h of polymerization, and the second is the main polymerization in micelles formed from the aggregation of the resultant block copolymers with the polymerization rate of 0.009 mol·L^{-1}·h^{-1}. The 2-bromoisobutyryl-terminated poly(ethylene glycol) methyl ether used in the polymerization acts as both a stabilizer and an initiator. The stable micelles with functional core were synthesized by a one-pot strategy via atom transfer radical dispersion copolymerization (ATRDCP) of 4VP and *N,N*′-methylenebisacrylamide (MBA) in an ethanol/H_2O solution for the first time. In the initial stage of polymerization, 4VP and MBA were copolymerized to form a block copolymer, PEG-*b*-(4VP-*co*-MBA), with pendent unreacted vinyl groups, and after phase separation at a critical chain length of P4VP-*co*-PMBA, the cross-linking reaction and polymerization occurred at the same time, resulting in cross-linked micelles. The volume ratio of ethanol/H_2O had a big influence on the ATRDCP. An increase in the relative amount of ethanol in the solvent mixture will increase the solubility of P4VP in the polymerization system, the phase separation will be postponed, and the critical chain length of 4VP blocks at the phase separation becomes longer. As a result, the particles size and the 4VP content in the resultant micelles increase. The Au/polymer composite nanoparticles were successfully prepared by complexation of P4VP with $HAuCl_4$ and following reduction with $NaBH_4$.

Introduction

Dispersion polymerization is a useful technique for preparation of micron and submicron particles with narrow size distribution and has attracted great attention from polymer chemists.[1,2] In a dispersion polymerization, all reaction ingredients are dissolved in a reaction medium at initial polymerization. As the polymerization progresses, the spherical polymer particles formed are stabilized by steric stabilizer and dispersed in the reaction medium homogeneously;[3] the polymerization then takes place mainly in the monomer-swollen droplet, and at last, a stable polymer latex is obtained. The stabilizer is necessary for dispersion polymerization so that monomer conversion higher than that in the precipitation polymerization can occur.[4] The stabilizer in the dispersed particles may be incompatible (or immiscible) with the polymer produced. Phase separation may occur in the resultant particles, possibly resulting in nonspherical particles and coagulation. In addition, the stabilizer cannot act as cross-linker when cross-linked particles are needed.[5] Removal of the stabilizer from the final polymeric particles is difficult and time-consuming. One way to solve these disadvantages is the copolymerization of the stabilizer with monomer, forming a pure polymer material.[6−8]

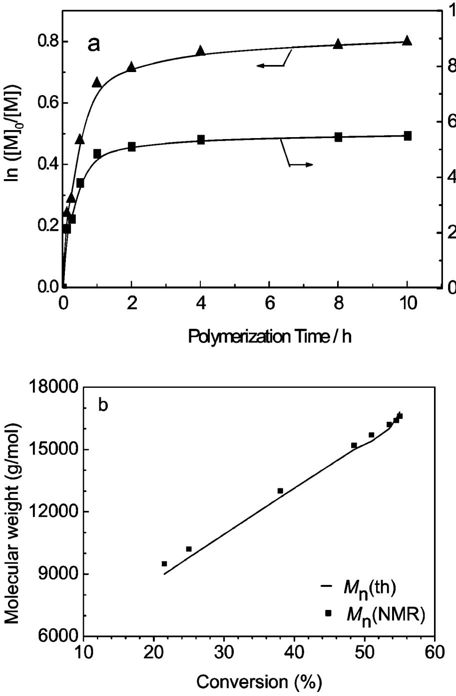

Figure 1. (a) The relationship of conversion and ln($[M]_0$/[M]) of 4-vinylpyridine (4VP) with polymerization time. (b) Variation of molecular weights [M_n(th) = theoretical molecular weight, M_n(NMR) = molecular weight was measured by NMR] with progress of conversion for the block copolymerization of 4VP using bromine-terminated poly(ethylene glycol) methyl ether (PEG-Br) as macroinitiator. Feed ratio of PEG-Br/4VP/CuBr/*N,N,N*′*,N*′*N*″-pentamethyldiethylenetriamine is 1:200:1:1, ethanol/H_2O = 1:1 (v/v), 60 °C. The conversion was calculated on the basis of ^{1}H NMR data.

Generally, dispersion polymerization is achieved via conventional free-radical chemistry. Recent years, several research groups have explored the application of living polymerization techniques in dispersion polymerization, and great progress has been achieved. The living polymerizations reported include anionic dispersion polymerization using poly(styrene-*block*-propylene-*alt*-ethylene) (PS-*b*-PP-*alt*-PE) or PS-*block*-polybutadiene (PS-*b*-PBD) as steric stabilizers,[9−12] group transfer polymerization in *n*-heptane with PS-*b*-PP-*alt*-PE as stabilizer,[13] and ring-opening polymerization of ϵ-caprolactone or L-lactide in mixed solvents.[14,15] However, these methods suffer from

---

* To whom all correspondence should be addressed. E-mail: pcy@ustc.edu.cn.

10.1021/ma0712854 CCC: $37.00

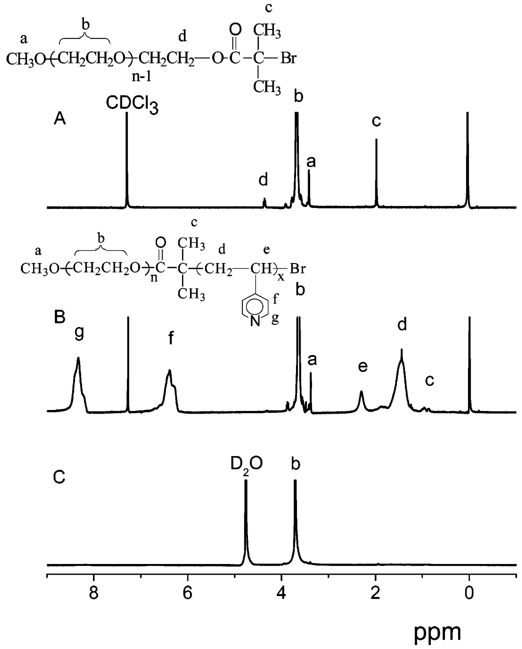

Figure 2. ^1H NMR spectroscopy of (A) bromine-terminated poly(ethylene glycol)methyl ether (PEG-Br), (B) PEG-*b*-poly(4-vinylpyridine)-(P4VP) in $CDCl_3$, and (C) PEG-*b*-4VP in D_2O. Polymerization conditions: 4VP/PEG-Br/*N*,*N*,*N*′,*N*′*N*″-pentamethyldiethylenetriamine/CuBr = 200:1:1:1 (molar ratio), ethanol/H_2O 1 mL:1 mL, 60 °C, 10 h.

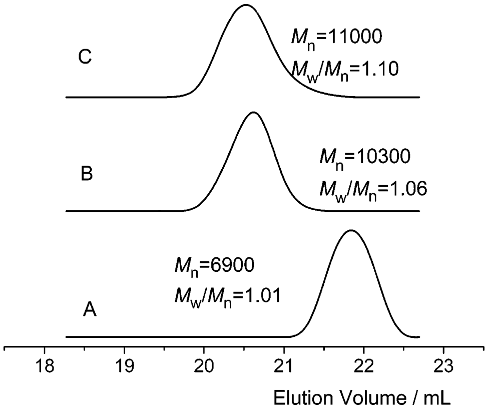

Figure 3. Gel permeation chromatography traces of (A) bromine-terminated poly(ethylene glycol)methyl ether (PEG-Br) and the block copolymers PEG-*b*-poly(4-vinylpyridine) (P4VP) obtained from polymerization in ethanol/H_2O (1:1, v/v) at 60 °C for different polymerization times: (B) 0.5 h and (C) 10 h. Feed molar ratio of 4VP/PEG-Br/CuBr/*N*,*N*,*N*′,*N*′,*N*″-pentamethyldiethylenetriamine = 200:1:1:1, ethanol/H_2O 1 mL:1 mL.

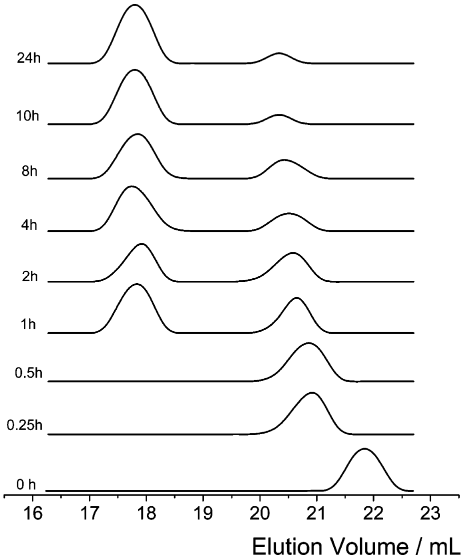

Figure 4. Gel permeation chromatography traces of the resultant polymers obtained from atom transfer radical dispersion copolymerization of 4-vinylpyridine (4VP) and *N*,*N*′-methylenebisacrylamide (MBA) at different polymerization times: 0 (PEG-Br), 0.25, 0.5, 1, 2, 4, 8, 10, and 24 h, respectively. Feed molar ratio of poly(ethylene glycol)methyl ether PEG-Br/4VP/MBA/CuBr/*N*,*N*,*N*′,*N*′*N*″-pentamethyldiethylenetriamine (PMDETA) is 1:200:10:1:1, ethanol/H_2O 1 mL:1 mL at 60 °C.

limited monomers and solvents and rigorous conditions.[16] Controlled radical polymerization (CRP) combines the merits of conventional radical and ionic living polymerizations, and advantages are the control of molecular weight, narrow molecular weight distribution, and tolerance of a variety of monomers, including functional monomers. The widely applied CRP techniques include stable free radical mediated polymerization,[17] atom transfer radical polymerization (ATRP),[18] and reversible addition−fragmentation chain transfer (RAFT) polymerization.[19] Nitroxide-mediated radical polymerization was used in the dispersion polymerization of styrene (St) and its derivatives in water/alcohol mixtures,[20] in *n*-decane using PS-*b*-PP-*alt*-PE as stabilizer,[21] or in *n*-octane, *n*-nonane, and *n*-dodecane using PS-*b*-PBD stabilizer.[22] The nitroxide-mediated radical dispersion polymerization in supercritical carbon dioxide was studied using poly(dimethylsiloxane-*b*-methyl methacrylate) (PDMS-*b*-PMMA)[23,24] or PDMS-*b*-PS as stabilizer.[25] In addition, application of RAFT polymerization in dispersion polymerization was investigated, for example, with RAFT dispersion polymerization of St in ethanol or in ethanol/water mixtures with 1-cyano-1-methylpropyl dithiobenzoate as RAFT agent[5] and dispersion photopolymerization of St in ethanol with various amount of RAFT agent using poly(*N*-vinylpyrrolidone) stabilizer.[3] Although controlled radical dispersion polymerizations have been studied extensively, no investigation on the atom transfer radical dispersion polymerization in water or water/alcohol mixtures was reported to our knowledge. In those polymerizations reported, the block copolymer without reactive group was used as stabilizer; the resultant products were contaminated with the stabilizer unavoidably. In addition, only common monomers, such as St and MMA, have been studied, and dispersion polymerization of functional monomers was not investigated. When the macromonomers are used in the controlled radical dispersion polymerization, the stabilizer contaminant in the resultant product may be solved. For example, RAFT polymerization using various macromonomers stabilizer has been studied, and the stable micelles were obtained.[26,27]

Among the numerous functional monomers, 4-vinylpyridine (4VP) is an interesting monomer. It is basic, nucleophilic, coordinating, and pH-sensitive. Its polymer, P4VP, is a weak polybase and can be dissolved in water only if the pyridine groups are highly protonated.[28] SFRP of 4VP was reported, and the polydispersities of the resultant polymers were relatively broad ($M_n/M_w \approx 1.2-1.5$).[29,30] However, ATRP of 4VP poses a challenging problem, because both 4VP and P4VP strongly coordinate copper ion, which will lead to a decrease of catalytic activity, and controlled radical polymerization cannot be achieved. Thus, strong binding ligands, such as tris[2-(dimethylamino)ethyl]amine, are needed for controlled radical polymerization.[31,32] In this paper, we studied the atom transfer radical dispersion polymerization (ATRDP) of 4VP using [poly(ethylene glycol) methyl ether] 2-bromoisobutyrate as initiator, and the morphology of the resultant products was investigated.

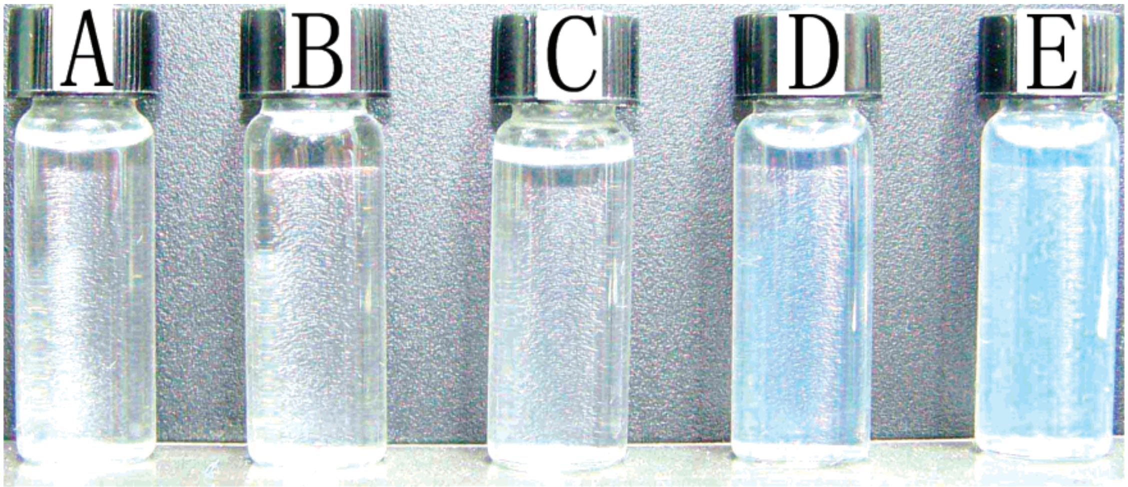

Figure 5. The photos of atom transfer radical dispersion polymerization of 4-vinylpyridine (4VP) and *N*,*N*′-methylenebisacrylamide (MBA) in ethanol/H_2O (1:1, v/v) at 60 °C for different polymerization times: (A) 0.25 h, (B) 0.5 h, (C) 1 h, (D) 2 h, and (E) 4 h. Feed molar ratio of bromine−terminated poly(ethylene glycol) methyl ether/4VP/MBA/CuBr/*N*,*N*,*N*′,*N*′*N*″-pentamethyldiethylenetriamine is 1:200:10:1:1, ethanol/H_2O 1 mL:1 mL.

Scheme 1. Formation of Nanosized Micelles and Atom Transfer Radical Dispersion Copolymerization of 4-Vinylpyridine (4VP) and *N*,*N*′-Methylenebisacrylamide (MBA) in Ethanol/H_2O Using Bromine-Terminated Poly(ethylene glycol) Methyl Ether (PEG-Br) As Macroinitiator

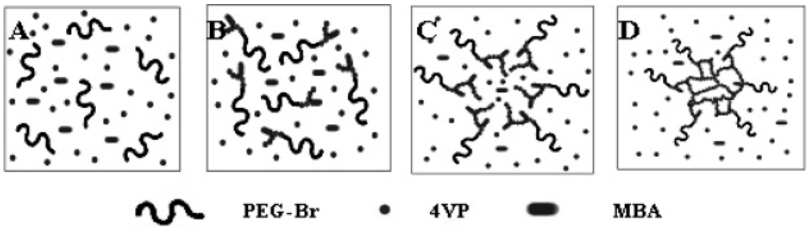

Experimental Section

Materials. CuBr (Shanghai Chemical Reagent Co, 99%) was purified by stirring in glacial acetic acid, washing with ethanol, and then drying in a vacuum oven at 70 °C overnight. 4-Vinylpyridine (Acros, 96%) was dried over CaH_2 and was distilled under reduced pressure prior to use. Poly(ethylene glycol) methyl ether ($M_n = 5000$ g mol^{-1}, Fluka), *N*,*N*′-methylenebisacrylamide (MBA, Aldrich), 2-bromoisobutyryl bromide (Aldrich, 98%), and other reagents with analytical grade were used as received. *N*,*N*,*N*′,*N*′*N*″-pentamethyldiethylenetriamine (PMDETA) was synthesized according to the procedures reported in ref 33.

Esterification Reaction of Poly(ethylene glycol) Methyl Ether with 2-Bromoisobutyryl Groups. The macroinitiator 2-bromoisobutyryl-terminated poly(ethylene glycol) methyl ether (PEG-Br) was synthesized according to the procedures reported.[34] Poly(ethylene glycol)methyl ether (MPEG, 10 g, 2 mmol) and anhydrous toluene (150 mL) were added into a 250 mL round-bottom flask equipped with a magnetic stirrer. After azeotropic distillation for removal of trace water, the mixture was cooled to 0 °C, and then triethylamine (TEA, 0.808 g, 8 mmol) was added. Subsequently, 2-bromobutyryl bromide (1.84 g, 8 mmol) was dropped in over 45 min, and a white precipitate of triethylammonium bromide formed immediately. The reaction solution was warmed to room temperature over approximately 2 h and was stirred for an additional 24 h. After the salt of TEA was filtered, the filtrate solution was concentrated under reduced pressure. The residue in CH_2Cl_2 was added into cold diethyl ether and the product was precipitated. The macroinitiator, PEG-Br, was obtained by filtration and then was dried in a vacuum oven at room temperature for 24 h. $CH_3O(CH_2CH_2O)_{113}COC(CH_3)_2Br$, M_n(GPC) = 6900. M_w/M_n = 1.01. ^{1}H NMR ($CDCl_3$, δ, ppm): 4.32 (t, 2H, $-CH_2OCO-$), 3.62 (m, 448H, $-OCH_2CH_2O-$), 3.3 (m, 3H, OCH_3), 1.94 (s, 6H, $2CH_3$).

Dispersion Polymerization of 4VP in Ethanol/H_2O (1:1, v/v) using the Macroinitiator PEG-Br. A typical polymerization procedure is as follows. The macroinitiator PEG-Br (0.129 g, 25 μmol), CuBr (3.6 mg, 25 μmol), PMDETA (4.55 mg, 25 μmol), 4VP (0.570 g, 5 mmol), ethanol (1 mL), and H_2O (1 mL) were successively added into a 5 mL glass tube with a magnetic bar, and then the system was degassed by three freeze−pump−thaw cycles. The tube was sealed under vacuum, and then the sealed tube was placed in an oil bath at 60 °C. After the polymerization was carried out for 10 h, the tube was opened. The reaction mixture was extracted three times with CH_2Cl_2 (3 × 20 mL); the extract was passed through a short neutral alumina column for removal of the copper complex. The eluent was concentrated using a rotary evaporator, and the residual liquid was added into excess diethyl ether. The precipitate was collected by filtration. After drying in a vacuum oven at 30 °C overnight, the white polymeric particles were obtained in 60% yield (0.421 g). M_n = 11 000 g/mol. M_w/M_n = 1.10. ^{1}H NMR ($CDCl_3$, δ, ppm): 8.34 (m, 110H, pyridine H ortho to N), 6.39 (m, 110H, pyridine H meta to N), 3.62 (m, 448H, $-OCH_2CH_2O-$), 3.3 (m, 3H, CH_3O), 2.01 (m, 55H, $-CH_2CH-$), 1.44 (m, 110H, $-CH_2CH-$), 0.98 (m, 6H, $2CH_3$).

For testing the kinetics of dispersion polymerization, the PEG-Br, CuBr, PMDETA, and 4VP with feed molar ratio of 1:1:1:200 were added into ethanol/H_2O (1:1, v/v) in the eight 5 mL glass tubes, respectively. The polymerizations were carried out under the same conditions mentioned above and then stopped at 8, 15, and 30 min and 1, 2, 4, 8, and 10 h, respectively. After the polymerization solution was treated with the same procedure mentioned above, white powder products were obtained in 32%, 35%, 45%, 53%, 55%, 57%, 59%, and 60% yields, respectively, by gravimetric method. On the basis of the integral values of signals at δ = 8.34 ($I_{8.34}$) and 3.62 ppm ($I_{3.62}$), corresponding to two pyridine protons and ether methylene protons of PEG, the conversions were calculated. The average molecular weights [M_n(NMR)s] of the resultant block copolymers were calculated on the basis of the integration ratio of $I_{8.34}$ to $I_{3.62}$, and they were 9500, 10 200, 13 000, 15 200, 15 700, 16 200, 16 400, and 16 600, respectively. ^{1}H NMR

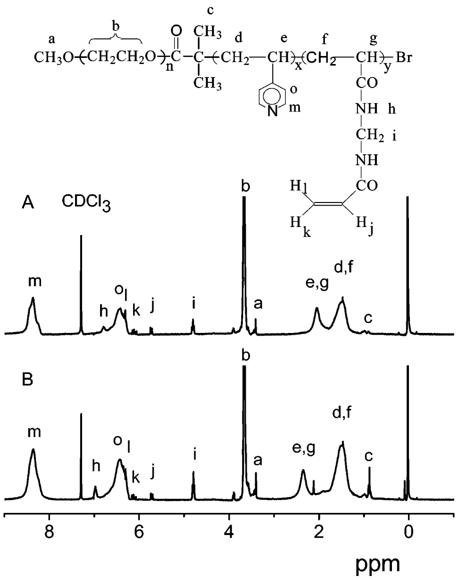

Figure 6. ^1H NMR spectroscopy of the resultant block copolymers obtained from atom transfer radical dispersion copolymerization of 4-vinylpyridine (4VP) and *N*,*N*′-methylenebisacrylamide (MBA) in ethanol/H_2O (1:1, v/v) at 60 °C using poly(ethylene glycol) methyl ether (PEG-Br) as macroinitiator at different polymerization times: (A) 0.5 h and (B) 10 h. Feed molar ratio of 4VP/MBA/PEG-Br/CuBr/*N*,*N*,*N*′,*N*′*N*′′-pentamethyldiethylenetriamine = 200:10:1:1:1.

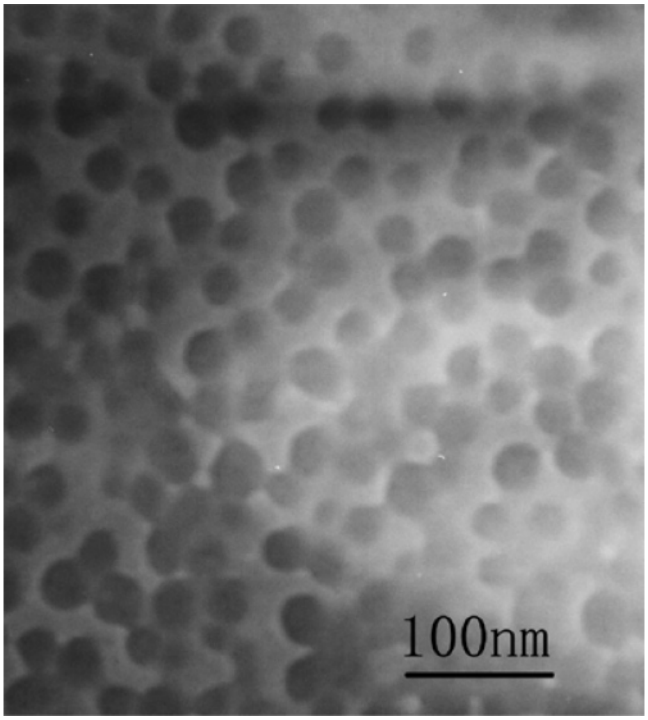

Figure 7. Transmission electron microscopy (TEM) photo of the resultant micelles formed from atom transfer radical dispersion copolymerization of 4-vinylpyridine (4VP) and *N*,*N*′-methylenebisacrylamide (MBA) (see sample 5 in Table 1).

($CDCl_3$, δ, ppm): 8.34 (m, pyridine H orthoto N), 6.39 (m, pyridine H meta to N), 3.62 (m, $-OCH_2CH_2O-$), 3.3 (m, CH_3O), 2.01 (m, $-CH_2CH-$), 1.44 (m, $-CH_2CH-$), 0.98 (m, $2CH_3$).

Dispersion Copolymerization of 4VP and MBA Using PEG-Br as Macroinitiator. A typical procedure is as follows. The PEG-Br (0.129 g, 25 μmol), CuBr (3.6 mg, 25 μmol), PMDETA (4.55 mg, 25 μmol), 4VP (0.570 g, 5 mmol), MBA (38.5 mg, 250 μmol), ethanol (1 mL), and H_2O (1 mL) were successively added into a 5 mL glass tube with a magnetic bar, and then the system was degassed by three freeze−pump−thaw cycles. The tube was sealed under vacuum, and then the sealed tube was placed in an oil bath at 60 °C with stirring. After polymerization was carried out for 24 h, the reaction mixture was cooled to room temperature. The tube was opened, the polymer solution was extracted three times with CH_2Cl_2 (3 × 20 mL), and the extract was passed through a short alumina column for removal of the copper complexes. The eluent solution was concentrated using a rotary evaporator, and the residual liquid was poured into excess diethyl ether. The precipitate was collected by filtration. After drying in a vacuum oven at 30 °C overnight, the white polymer particles (0.443 g) were obtained in 60% yield. ^1H NMR ($CDCl_3$, δ, ppm): 8.34 (m, pyridine H ortho to N), 6.77 (m, $-NHCH_2NH-$), 6.39 (m, pyridine H meta to N), 6.36, 6.12 (m, $CH_2{=}CH$), 5.70(m, $CH_2{=}CH$), 4.79 (m, $-NHCH_2$-NH−), 3.62 (m, $-OCH_2CH_2O-$), 3.3 (m, CH_3O), 2.01 (m, $-CH_2CH-$), 1.44 (m, $-CH_2CH-$), 0.98 (m, $2CH_3$).

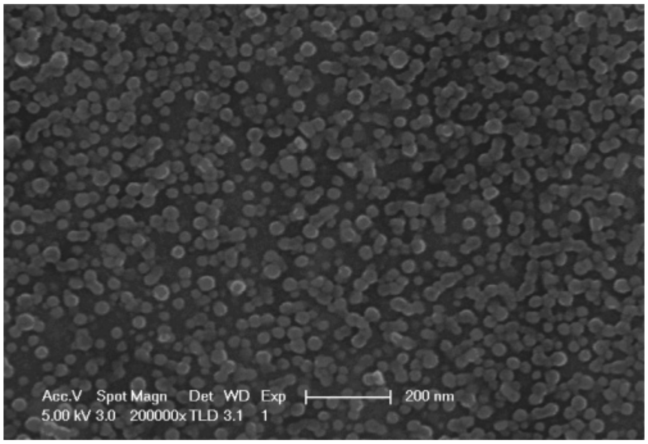

Figure 8. Field emission scanning electron microscopy image of the resultant micelles (sample 5 in Table 1) prepared from the atom transfer radical dispersion copolymerization.

To study the effect of the polymerization time on the dispersion polymerization, the polymerizations with the same feed molar ratio of PEG-Br/CuBr/PMDETA/MBA/4VP = 1:1:1:10:200 were carried out respectively in the eight 5 mL glass tubes under the same polymerization conditions mentioned above, and then the polymerization was stopped at 0.25, 0.5, 1, 2, 4, 8, 10, and 24 h, respectively. After polymerization solutions were treated with the same procedure mentioned above, the white polymer particles were obtained in 34%, 37%, 47%, 55%, 57%, 58%, 59%, and 60%, respectively.

Influence of the Ethanol/H_2O Ratio on the Dispersion Polymerization of 4VP and MBA Using Macroinitiator PEG-Br. After PEG-Br, PMDETA, 4VP, and MBA were dissolved in ethanol/H_2O mixture homogeneously, the solution was divided equally into five portions. Each portion contained PEG-Br (0.129 g, 25 μmol), PMDETA (4.55 mg, 25 μmol), 4VP (0.570 g, 5 mmol), and MBA (38.5 mg, 250 μmol). Those five portions were added into five 5 mL glass tubes. Separately, CuBr (3.6 mg, 25 μmol) and 2 mL of ethanol/H_2O with various volume ratios of 1/1, 1/1.5, 1/2, 1/3, and 0/1 (v/v) were added into each glass tube, and then the system was degassed by three freeze−pump−thaw cycles. The tubes were sealed under vacuum and then placed in an oil bath at 60 °C with stirring. After 10 h of polymerization, the tube was cooled to room temperature and then opened. The reaction mixture was extracted with CH_2Cl_2, and the resultant organic solution was passed through a short neutral alumina column for removal of the copper complex. The eluent solution was concentrated using a rotary evaporator, and the residual liquid was poured into excess of diethyl ether. The precipitate was collected by filtration, and the target polymer particles were obtained after dried in a vacuum oven at 30 °C overnight. The R_hs of micelles are 29.8, 24.7, 22.1, gelation, and gelation, respectively. ^1H NMR ($CDCl_3$, δ, ppm): 8.34 (m, pyridine H ortho to N), 6.77 (m, $NHCH_2NH$), 6.39 (m, pyridine H meta to N), 6.36, 6.12 (m, $CH_2{=}CH$), 5.70 (m, $CH_2{=}CH$), 4.79 (m, $-NHCH_2NH-$), 3.62 (m, $-OCH_2CH_2O-$),

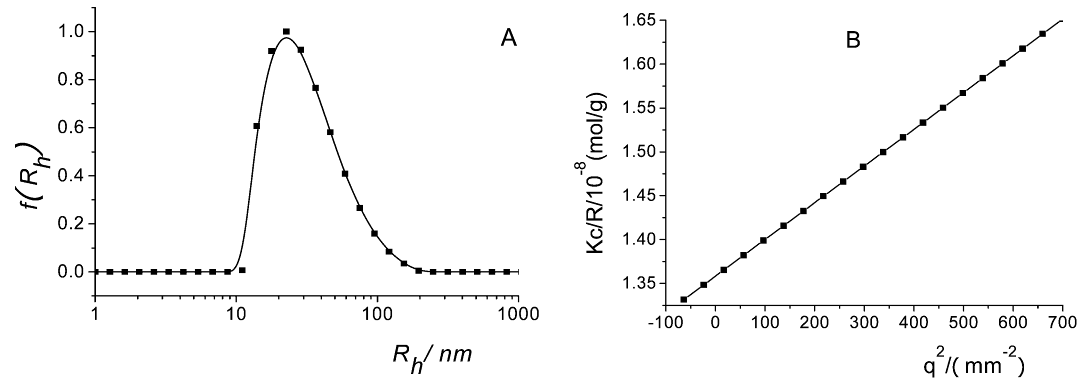

Figure 9. (A) Hydrodynamic radius distribution (R_h) and (B) *z*-average root-mean square radius of gyration (R_g) of the micelles prepared from sample 5 in Table 1, which were measured by dynamic light scattering (DLS) and static light scattering (SLS) at 25 °C.

Scheme 2. Preparation of Micelles by Polymer Linking Reaction

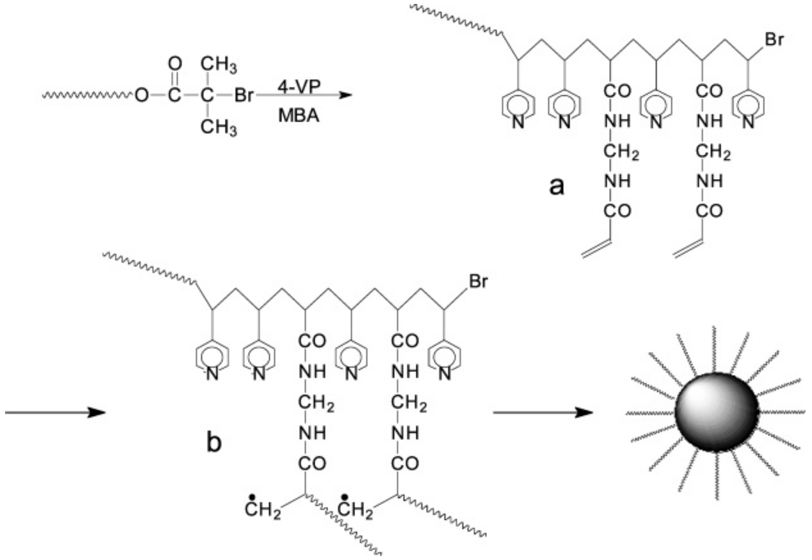

3.3 (m, CH_3O), 2.01 (m, $-CH_2CH-$), 1.44 (m, $-CH_2CH-$), 0.98 (m, 2CH_3).

Coordination of the Polymer Particles with $HAuCl_4$. The resultant polymer particles were dissolved in ethanol to form a transparent polymer solution with a concentration of 1 mg/mL. $HAuCl_4$ solution in ethanol (1 mg/mL) was dropped into this solution under nitrogen atmosphere with stirring. In order to study the effect of feeding ratio of $HAuCl_4$ on the morphology of the micelles, molar ratios of 0.5:1, 1:1, 1.5:1, and 2:1 were investigated. After coordinating reaction was carried out at room temperature for 2 days, $NaBH_4$ aqueous solution with concentration of 1 mg/mL was dropped in.

Characterization. *Nuclear Magnetic Resonance (NMR) Spectroscopy.* The ^{1}H NMR (300 MHz) measurements were performed on Bruker DMX300 spectrometer in $CDCl_3$ or in D_2O using tetramethylsilane as an internal reference.

Gel Permeation Chromatography. The molecular weight and molecular weight distribution were determined on a Waters 150C gel permeation chromatograph (GPC) equipped with three Ultrastyragel columns (500, 10^3, 10^4Å) in series and RI 2414 detector at 30 °C, and tetrahydrofuran (THF) was used as eluent at a flow rate of 1.0 mL/min. Monodisperse polystyrene was used to calibrate molecular weight and molecular weight distribution.

Field Emission Scanning Electron Microscopy. The field-emission scanning electron microscope (FESEM) images were measured on a JEOL JSM-6700F. The samples were prepared by placing a drop of the polymer solution in ethanol on copper grids and gilding a shell of Pt nanoparticle.

Transmission Electron Microscopy. The transmission electron microscope (TEM) observations were performed on a Hitachi H-800 microscope at an accelerating voltage of 200 kV. The samples for TEM observations were prepared by depositing a drop of the polymer solution in ethanol on copper grids.

High-Resolution Transmission Electron Microscopy (HRTEM). HRTEM images were carried out on a JEOL JEL2010 electron microscope at 200 kV acceleration voltage. The same procedure with TEM observations was used for preparation of samples.

UV−Vis Spectra. The UV−vis spectra were recorded on a Hitachi U-3010 spectrophotometer (Japan) in the range of 200−800 nm.

Laser Light Scattering (LLS). LLS studies were conducted on a modified commercial LLS spectrometer (ALV/DLS/SLS-5022F) equipped with a ALV-5000 multi-τ digital time correlator and a cylindrical 22 mW UNIPHASE He−Ne laser ($\lambda_0 = 532$ nm) as the light source. In static LLS, we can obtain the *z*-average root-mean square radius of gyration ($\langle R_g \rangle$) of polymer chains in a dilute solution from the angular dependence of the excess absolute scattering intensity, known as Rayleigh ratio $R_{vv}(q)$, which is dependent on the scattering vector q

$$\frac{KC}{R_{vv}(q)} \approx \frac{1}{M_w}\left(1 + \frac{1}{3}\langle R_g{}^2\rangle q^2\right) + 2A_2C \qquad (1)$$

where $K = 4\pi^2 n^2 (dn/dc)^2/(N_A \lambda_0{}^4)$ and $q = (4\pi n/\lambda_0)\sin(\theta/2)$, with N_A, dn/dc, n, and λ_0 being Avogadro's number, the specific refractive index increment, the solvent refractive index, and the wavelength of the laser light in a vacuum, respectively, and A_2 is the second virial coefficient. Strictly speaking, here $R_{vv}(q)$ should be $R_{vu}(q)$ because there is no analyzer before the detector. However, the depolarized scattering of the solution studied is insignificant so that $R_{vu}(q) \approx R_{vv}(q)$. In dynamic LLS, the Laplace inversion of

Table 1. Conditions and Results for Atom Transfer Radical Dispersion Polymerization of 4-Vinylpyridine (4VP) and *N*,*N*′-Methylenebisacrylamide (MBA) in Various Ratios of Ethanol/H_2O^a

sample	ethanol:H_2O (v/v)	time (h)	conversion (%)^b	$R_h{}^c$ (nm)	size distribution^c	composition of MPEG-*b*-P4VP^d
1	0:1	0.08	gelatin			
2	1:3	1.5	gelatin			
3	1:2	10	44	22.1	0.204	113:94
4	1:1.5	10	51	24.7	0.177	113:109
5	1:1	10	55	29.8	0.231	113:115

[a] Feed ratio = $[4VP]_0/[MBA]_0$/[poly(ethylene glycol) methyl ether (MPEG)-Br]$_0$/[CuBr]/[*N*,*N*,*N*′,*N*′*N*″-pentamethyldiethylenetriamine (PMDETA)] = 200:10:1:1:1 (molar ratio); 4VP, 0.570 g; ethanol/H_2O, 2 mL; temperature, 60 °C. [b] Conversions were measured by the gravimetric method. [c] Hydrodynamic radius (R_h) and size distribution were obtained from dynamic light scattering. [d] Composition of MPEG-*b*-P4VP was calculated by ^{1}H NMR spectroscopy.

each measured intensity−intensity−time correlation function $G^{(2)}(q,t)$ can lead to a line-width distribution $G(\Gamma)$. For a pure diffusive relaxation, Γ is related to the translational diffusion coefficient D by $D = (\Gamma/q^2)_{q\to 0, C\to 0}$, or further to the hydrodynamic radius R_h via the Stokes−Einstein equation, $R_h = (k_BT/6\pi\eta D)$, where k_B, T, and η are the Boltzmann constant, the absolute temperature, and the solvent viscosity, respectively. Therefore, $G(\Gamma)$ can be converted to a hydrodynamic radius distribution $f(R_h)$. The CONTIN Laplace inversion program in the correlator was used. All the static and dynamic LLS measurements were done at 25 °C.

Results and Discussion

Atom Transfer Radical Dispersion Polymerization of 4VP Using PEG-Br as Initiator. The controlled radical dispersion polymerization of conventional monomers, such as St and MMA, using block copolymer as stabilizer has been studied.[20−25] In this study, PEG-Br was used as an inistab, which acts as both initiator and stabilizer, instead of block copolymer. In addition, we selected PMDETA as ligand for improving the controlled nature of 4VP polymerization. Therefore, the atom transfer radical dispersion polymerization (ATRDP) of 4VP in ethanol/H_2O (1:1, v/v) was followed by the ^{1}H NMR method. The conversions of 4VP at different polymerization time were calculated on the basis of the integration ratio of signals of P4VP at $\delta = 8.34$ and 6.39 ppm to the signals of PEG at $\delta = 3.64$, 3.39 ppm. Figure 1a shows the relationship of conversion and $\ln([M]_0/[M])$ with polymerization time. Different from conventional radical dispersion polymerization behavior using block copolymer as stabilizer, in which the polymerization rate was leveled off until conversion higher than 90%,[34] the polymerization was fast in the first 1 h (1.21 mol·L^{-1}·h^{-1}), which is similar to the phenomenon of ATRP in the presence of H_2O, which was extremely rapid;[35,36] possibly water can help to dissolve the catalyst. The following polymerization rate (0.009 mol·L^{-1}·h^{-1}) was slowed down suddenly. The turning point at 1 h might reflect the variation of the polymerization mechanism. Consider that the solvent mixture is a good solvent for both 4VP and PEG but is a nonsolvent for P4VP. At the beginning of polymerization, the polymerization system was homogeneous, and the PEG-Br initiated the polymerization of 4VP with the aid of CuBr/PMDETA. The ATRP proceeded to form block copolymer, PEG-*b*-P4VP. With the chain length increase of P4VP to a critical value, phase separation occurred to form micelles with PEG shell and P4VP core. The evidence for this explanation is that, at the last stage of polymerization, the polymerization system displayed faint blue opalescence, indicating the formation of nanosized microspheres. Further polymerization proceeded in the micelles, and the polymerization became slow due to the difficult diffusion of 4VP monomer from solution to the micelles, which will be explained later. The linear relationship of M_n(NMR) with conversion in Figure 1b indicates that the polymerization can be controlled by feed molar ratio and conversion, and M_n(NMR) values are accordant with the theoretical molecular weights. The formation of block copolymers in the ATRDP can be confirmed by their ^{1}H NMR spectra. Figure 2B is the ^{1}H NMR spectrum of the polymer obtained from ATRDP of 4VP. For comparison, the ^{1}H NMR spectrum of PEG-Br is shown in Figure 2A also. We can find the characteristic signals of PEG at $\delta = 3.64$ (b) and 3.39 ppm (a) and that of P4VP at $\delta = 8.34$ (g) and 6.39 ppm (f). On the basis of their integration ratio, the composition of the copolymer was calculated and it is poly[$(EG)_{113}$-*b*-$(4VP)_{110}$]. Their GPC traces of the PEG-Br and PEG-*b*-P4VP are shown in Figure 3. The unimodal and symmetrical GPC curves demonstrate that those polymers are not mixture of the two polymers, verifying further the formation of block copolymers.

Atom Transfer Radical Dispersion Copolymerization of 4VP and MBA in Ethanol/H_2O. For getting stable micelles, atom transfer radical dispersion copolymerization (ATRDCP) of 4VP with MBA as cross-linker and PEG-Br as initiator was carried out in the ethanol and water mixture. At first, the GPC method was used to follow the polymerization in order to understand the ATRDCP process. Figure 4 shows the GPC traces of PEG-Br and the polymer products obtained at different polymerization times. The ATRDCP process can be explained by Scheme 1. At the beginning of polymerization, the starting materials are dissolved in the ethanol/H_2O, forming a homogeneous solution (Scheme 1A). Before 1 h of polymerization, only unimodal GPC traces were observed, and with the progress of polymerization, the GPC curves were shifted to high molecular weight position due to the molecular weight increase of the 4VP-*co*-MBA blocks in the block copolymers. Thus, the block copolymers PEG-*b*-P(4VP-*co*-MBA) were formed as shown in Scheme 1B. At this stage, the polymerization solution was transparent, as shown in Figure 5A,B, and no phase separation had taken place. The narrow molecular weight distribution ($M_w/M_n = 1.07$) of the polymers formed may have resulted from the intactness of the secondary vinyl groups of MBA units in the 4VP-*co*-MBA blocks, except the living nature of ATRP; this was confirmed by the ^{1}H NMR spectrum of the block copolymer obtained at 0.5 h of polymerization in Figure 6A, and we can see the vinyl protons signals at $\delta = 5.70$ (j), 6.12 (k), and 6.36 (l) ppm. On the basis of the degree of polymerization of PEG-Br and the integral values of the signal at $\delta = 3.64$ and 5.70 ppm, we estimated that there are two intact secondary vinyl groups per initial PEG-Br chain. The resultant block copolymer is of the structure shown in Scheme 2a, which is similar to the result reported.[37] At 1 h of polymerization, two GPC traces of the resultant polymers were observed; the one at the lower molecular weight position is the PEG-*b*-(4VP-*co*-MBA) block, and other at the high molecular weight position is the micelles that were formed by self-assembly of the resultant block copolymers. Probably, at this point the chain length of the P4VP-*co*-MBA blocks reached the critical value, and the aggregation occurred to form micelles with a P4VP-*co*-MBA

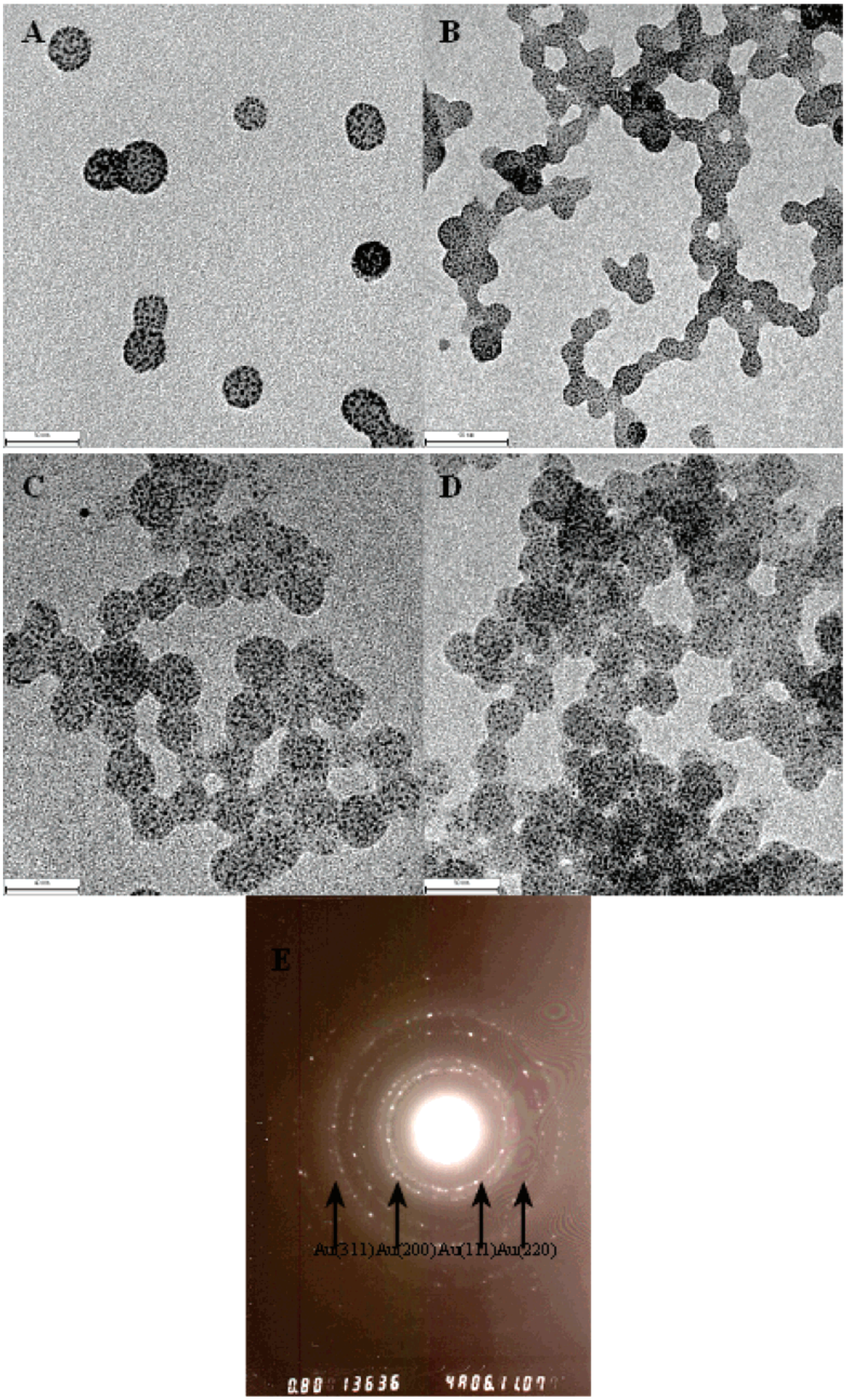

Figure 10. The high-resolution transmission electron microscopy of the Au/micelles composite particles prepared from reduction of $HAuCl_4$ in micelles (sample 5 in Table 1) by $NaBH_4$ with different feeding molar ratios of $HAuCl_4$ to micelles: (A) 0.5:1, (B) 1:1, (C) 1.5:1, and (D) 2:1. Scale bars are 50, 90, 40, and 50 nm, respectively. (E) The electron diffraction of Au in the composite particles.

core and PEG shell due to the poor solubility of P4VP-*co*-MBA in the polymerization media (Scheme 1C). The polymerization solution formed at 1 h displayed a faint blue opalescence, as shown in Figure 5C. The cross-linking reaction between the block copolymer chains as shown in Scheme 2b will help to form the micelles. The following polymerization and cross-linking reactions were underwent mainly in the micelles formed, as shown in Scheme 1D. With the progress of polymerization, the polymerization system gradually became faintly milky, as shown in Figure 5D,E, and the GPC traces of the block

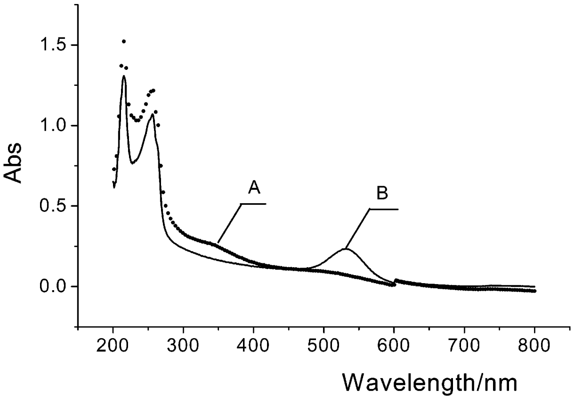

Figure 11. UV−vis spectra of (A, dot) the micelles formed from sample 5 in Table 1 and (B, line) the Au/polymer composite particles; solvent, ethanol; concentration, 0.5 mg/mL; temperature, 25 °C.

copolymer chains in Figure 4 shifted to high molecular weight position continuously, that is, the chain lengths of block copolymer chains increased. Thus, the PEG-*b*-(4VP-*co*-MBA) chains propagated and precipitated onto the micelles continuously; we can observe that with evolution of the polymerization, the area of the high molecular weight trace increased, and the block copolymer trace decreased.

The cross-linking reaction in the micelles was confirmed by their ^{1}H NMR spectra. Figure 6B shows the ^{1}H NMR spectrum of the resultant polymer obtained from ATRDCP at 10 h of polymerization. In comparison with Figure 6A, the proton signals are the same, although their relative integration values are different. For estimating the progress of cross-linking reaction, the proton signal at $\delta = 4.78$ ppm, which corresponds to the methylene group between two amides in MBA, was used as reference. In the ^{1}H NMR spectrum of the polymer obtained from 0.5 h of polymerization (Figure 6A), the integration ratio of one vinyl proton signal at $\delta = 5.70$ ppm (j) to the signal at $\delta = 4.78$ ppm (i) is 1:1.93, which is close to 1:2. This verifies further that the second vinyl group of MBA did not participate in polymerization. For the polymer obtained from 10 h of polymerization, Figure 6B shows that this ratio decreased to 1:5.42, less than the theoretical value of 1:2, indicating the occurrence of the cross-linking reaction to form particles with 4.78 cross-linking points per block chain, calculated on the basis of the integral values of signals at $\delta = 4.78$, 5.70, and 3.63 ppm, as well as the degree of polymerization of PEG-Br.

The Effect of the Volume Ratio of Ethanol/H_2O on the Dispersion Polymerization of 4VP and MBA Using PEG-Br as Macroinitiator. For P4VP, ethanol is a solvent, but H_2O is a nonsolvent, which can be confirmed by the ^{1}H NMR spectrum of PEG-*b*-P4VP in D_2O shown in Figure 2C. Only characteristic signals of PEG and no characteristic protons signals of P4VP appeared in Figure 2C. This demonstrates that the water-soluble PEG blocks form a shell and the P4VP blocks are aggregated to form core, due to the insolubility of P4VP in D_2O. Therefore, the ratio of ethanol to H_2O is an important factor influencing the dispersion polymerization of 4VP and MBA using PEG-Br as macroinitiator. So the ATRDP in ethanol/H_2O mixtures with various volume ratios was studied. The results and conditions are listed in Table 1. We observed that when the water was used as polymerization media, gelation occurred in 5 min, because the PEG-Br initiated the polymerization of water-soluble MBA mainly, and gelation happened very fast due to the fast polymerization in water. When the volume ratio of ethanol/H_2O was changed to 1:3, the gelation was delayed to 1.5 h of polymerization. When the amount of ethanol in the mixture solvent increased continuously from the volume ratio of ethanol/H_2O = 1:2 to 1:1.5 to 1:1, no gelation was observed, even after 10 h of polymerization. Increasing the relative amount of ethanol in the mixture solvent will increase the solubility of P4VP. The phase separation will be postponed, and the critical chain length of 4VP blocks at the phase separation becomes longer. It is favorable to increase the 4VP content in the target polymers.

Characterization of the Micelles. We call the products synthesized in this study micelles, not star polymers, because the resultant particles are expected to be spherical, and their cores are bigger than their coronas, due to their lightly cross-linked cores and linear PEG shells. To verify the spherical particles and incompact cores of micelles obtained from ATRDCP of 4VP and MBA in ethanol and water mixture, TEM, FESEM, and DLS/SLS measurements were carried out. The sample 5 in Table 1 was used in all tests. One typical TEM image is shown in Figure 7. All particles were spherical, and their number-average diameter is 30.5 nm, which was calculated on the basis of the measurements of 80 particles. The FESEM image is shown in Figure 8. With the same calculation method for particles size based on TEM image, the number-average diameter of micelles is 33.4 nm, which matches the TEM result. In order to verify the incompact core structure of the resultant micelles, DLS/SLS measurements were performed in ethanol. The results in Figure 9A show that $\langle R_h \rangle$ of the micelles is 29.8 nm and PDI = 0.231, and from SLS results in Figure 9B, the $\langle R_g \rangle$ of the micelles is 30.6 nm. So the ratio of $\langle R_g \rangle / \langle R_h \rangle = 1.03$. As mentioned in the literature,[38,39] the $\langle R_g \rangle / \langle R_h \rangle$ values for the polymer coils, uniform spheres, and thin-layer hollow spheres or incompact structure are 1.50, 0.77, and 1.0, respectively. Thus, the micelles prepared from one-pot synthesis via ATRDCP have an incompact structure corresponding to the low cross-linking degree of the core, and the micelles were swollen during measurement.

Coordination of the Micelles with $HAuCl_4$. As aforementioned in the introduction, the P4VP is a strong coordination ligand, which can be coordinated with metal ions. Therefore, the complexation of P4VP in the cores of micelles with $HAuCl_4$ was investigated. Figure 10 is the HRTEM images of the Au/polymer composite particles prepared from sample 5 in Table 1 and $HAuCl_4$ with molar ratios of polymer micelles to $HAuCl_4$ = 0.5:1, 1:1, 1.5:1, and 2:1 in ethanol followed by reduction with $NaBH_4$. We can see that very fine Au particles with 1.6 nm in diameter were embedded in the polymer micelles homogeneously. Electron diffraction in Figure 10E displays the typical crystal structure of Au nanoparticles. The diffraction rings and spots can be indexed as 111, 200, 220, and 311 of face-center-cubic Au polycrystallites. With the increase of $HAuCl_4$ in the feed, the composite particles tend to be connected to each other to form a chainlike structure (see Figure 10B−D). Probably, the complexation of Au with oxygen in PEG may occur, although the complexing ability of oxygen is lower in comparison with nitrogen. When the quantity of Au is low, the coordination between nitrogen atom and Au mainly happened, retaining the morphology of the starting micelles. As the concentration of $HAuCl_4$ increased, coordination of excess Au with the oxygen atom may occur, and more and more Au/polymer composite particles were connected each other, forming the various morphologies shown in Figure 10C,D. Spherical Au nanoparticles can be verified further by their UV−vis spectra, and Figure 11B is the absorbance spectrum of Au/polymer composite particles. For comparison, the UV−vis spectrum of the polymer micelles formed from sample 5 in Table 1 is shown in Figure 11A. In addition to the absorbance bands of polymer, an absorbance band at 532 nm, which is characteristic of spherical Au nanoparticles,[40] can be found in Figure 11B.

Conclusion

The kinetic study for the ATRDP of 4VP in ethanol/H_2O mixture (1/1, v/v) using PEG-Br initiator demonstrated two stages of polymerization, the first stage of polymerization with the rate of 1.21 $mol{\cdot}L^{-1}{\cdot}h^{-1}$ proceeded before 1 h polymerization, and the subsequent polymerization rate (0.009 $mol{\cdot}L^{-1}{\cdot}h^{-1}$) was slowed down. For the ATRDCP of 4VP and MBA in ethanol/H_2O using PEG-Br initiator, the block copolymer PEG-*b*-(4VP-*co*-MBA) was formed before 1 h polymerization, and then aggregation of the block copolymer molecules formed micelles with P4VP-*co*-MBA as core and PEG as shell. Subsequent polymerization in the micelles produced stable micelles, which were verified by TEM, FESEM, DLS, and SLS measurements. Thus, the stable micelles with P4VP core and PEG shell have been successfully prepared in the ethanol/H_2O (1:1, v/v) with a concentration of about 150 mg/mL by one-pot synthesis via ATRDP. The volume ratio of ethanol to H_2O has a big influence on the ATRDCP, and when the ratio of ethanol/H_2O was lower than 1:2, a gel was formed easily. Au/polymeric composite nanoparticles were prepared by complexation of P4VP with $HAuCl_4$ followed by reduction with $NaBH_4$. Their UV−vis spectrum shows a translational surface plasmon band at 532 nm, characteristic of spherical Au nanoparticles.

Acknowledgment. This work is supported by the National Natural Science Foundation of China under Contract No. 50673086 and 50633010.

References and Notes

(1) Barrett, K. E. J. *Dispersion Polymerization in Organic Media;* Wiley: New York, 1975.
(2) Ober, C. K.; Lok, K. P. *Macromolecules* **1987**, *20*, 268−273.
(3) Shim, S. E.; Jung, H.; Lee, H.; Biswas, J.; Choe, S. *Polymer* **2003**, *44* (19), 5563−5572.
(4) Srinivasan, S. A.; Hedrick, J. L.; McKean, D. R.; Miller, R. D.; Hilbom, J. G. *Polymer* **1998**, *39* (6−7), 1497−1501.
(5) Song, J. S.; Winnik, M. A. *Macromolecules* **2006**, *39*, 8318−8325.
(6) Kawaguchi, S.; Winnik, M. A.; Ito, K. *Macromolecules* **1996**, *29*, 4465−4472.
(7) Gibanel, S.; Heroguez, V.; Forcada, J.; Gnanou, Y. *Macromolecules* **2002**, *35*, 2467−2473.
(8) Yildiz, U. *Macromol. Symp.* **2002**, *179*, 297−304.
(9) Schwab, F. C.; Murray, J. G. *Polym. Sci. Technol.* **1985**, *31*, 381−404.
(10) Jenkins, A. D.; Maxfield, D.; Dossantos, C. G.; Walton, D. R. M.; Stejskal, J.; Kratochvil, P. *Makromol. Chem. Rapid Commun.***1992**, *13*, 61−63.
(11) Awan, M. A.; Dimonie, V. L.; ElAasser, M. S. *J. Polym. Sci. Part A: Polym Chem* **1996**, *34*, 2651−2664.
(12) Kim, J.; Jeong, S. Y.; Kim, K. U.; Ahn, Y. H.; Quirk, R. P. *J. Polym. Sci. Part A: Polym. Chem.* **1996**, *34*, 3277−3288.
(13) Awan, M. A.; Dimonie, V. L.; ElAasser, M. S. *J. Polym. Sci. Part A: Polym. Chem.* **1996**, *34*, 2633−2649.
(14) Gadzinowski, M.; Sosnowski, S.; Slomkowski, S. *Macromolecules* **1996**, *29*, 6404−6407.
(15) Sosnowski, S.; Gadzinowski, M.; Slomkowski, S. *Macromolecules* **1996**, *29*, 4556−4564.
(16) Matyjaszewski, K. *Cationic Polymerizations: Mechanisms, Synthesis & Applications*; Marcel Dekker: New York, 1996.
(17) Georges, M. K.; Veregin, R. P. N.; Kazmaier, P. M.; Hamer, G. K. *Macromolecules* **1993**, *26*, 2987−2988.
(18) Wang, J. S.; Matyjaszewski, K. *J. Am. Chem. Soc.* **1995**, *117*, 5614−5615.
(19) Chiefari, J.; Chong, Y. K.; Ercole, F.; Krstina, J.; Jeffery, J.; Le, T. P. T.; Mayadunne, R. T. A.; Meijs, G. F.; Moad, C. L.; Moad, G.; Rizzardo, E.; Thang, S. H. *Macromolecules* **1998**, *31*, 5559−5562.
(20) Keoshkerian, B.; Georges, M. K.; Boilsboissier, D. *Macromolecules* **1995**, *28*, 6381−6382.
(21) Holderle, M.; Baumert, M.; Mulhaupt, R. *Macromolecules* **1997**, *30*, 3420−3422.
(22) Gabaston, L. I.; Jackson, R. A.; Armes, S. P. *Macromolecules* **1998**, *31*, 2883−2888.
(23) Ryan, J.; Aldabbagh, F.; Zetterlund, P. B.; Okubo, M. *Polymer* **2005**, *46*, 9769−9777.
(24) McHale, R.; Aldabbagh, F.; Zetterlund, P. B.; Minami, H.; Okubo, M. *Macromolecules* **2006**, *39*, 6853−6860.
(25) McHale, R.; Aldabbagh, F.; Zetterlund, P. B.; Okubo, M. *Macromol. Rapid Commun.* **2006**, *27*, 1465−1471.
(26) Zheng, G. H.; Pan, C. Y. *Macromolecules* **2006**, *39*, 95−102.
(27) Zheng, G. H.; Pan, C. Y. *Acta Polym. Sin.* **2005**, (5), 664−668.
(28) Tsarevsky, N. V.; Braunecker, W. A.; Brooks, S. J.; Matyjaszewski, K. *Macromolecules* **2006**, *39*, 6817−6824.
(29) Bohrisch, J.; Wendler, U.; Jaeger, W. *Macromol. Rapid Commun.* **1997**, *18*, 975−982.
(30) Baumann, M.; Schmidt-Naake, G. *Macromol. Chem. Phys.* **2000**, *201*, 2751−2755.
(31) Xia, J. H.; Zhang, X.; Matyjaszewski, K. *Macromolecules* **1999**, *32*, 3531−3533.
(32) Yang, R. M.; Wang, Y. M.; Wang, X. G.; He, W. D.; Pan, C. Y. *Eur. Polym. J.* **2003**, *39*, 2029−2033.
(33) Queffelec, J.; Gaynor, S. G.; Matyjaszewski, K. *Macromolecules* **2000**, *33*, 8629−8639.
(34) Gibanel, S.; Heroguez, V.; Forcada, J.; Gnanou, Y. *Macromolecules* **2002**, *35*, 2467−2473.
(35) Wang, X. S.; Armes, S. P. *Macromolecules* **2000**, *33*, 6640−6647.
(36) Wang, X. S.; Jackson, R. A.; Armes, S. P. *Macromolecules* **2000**, *33*, 255−257.
(37) Baek, K. Y.; Kamigaito, M.; Sawamoto, M. *Macromolecules* **2001**, *34*, 215−221.
(38) Dou, H. j.; Jiang, M.; Peng, H. S.; Chen, D. Y.; Hong, Y. *Angew. Chem., Int. Ed.* **2003**, *42*, 1516−1519.
(39) Zhou, S. Q.; Wu, C. *Phys. Rev. Lett.* **1996**, *77*, 3053−3055.
(40) McGilvray, K. L.; Decan, M. R.; Wang, D.; Scaiano, J. C. *J. Am. Chem. Soc*. **2006**, *128*, 15980−15981

MA0712854